Insights into Probing the Effect of Molecular Weight of Poly(carboxybetaine methacrylate) on the Performance of Forward Osmosis Desalination

Jessika Pazol[1, 2], Xiao Tong[3], Gregory S. Doerk[3], Dina Bracho[4], Samir A. Bello[1, 2], Luarys Díaz-Fuentes[1], and Eduardo Nicolau[1, 2]*

[1] Department of Chemistry, University of Puerto Rico, Rio Piedras Campus, 17 Ave. Universidad Ste. 1701, San Juan, Puerto Rico USA 00925-2537

[2] Molecular Sciences Research Center, University of Puerto Rico, 1390 Ponce De León Ave, Suite 2, San Juan Puerto Rico USA 00931-3346

[3] Center for Functional Nanomaterials, Brookhaven National Laboratory, Upton, New York 11973, United States

[4] Institute of Neurobiology, University of Puerto Rico, Medical Sciences Campus San Juan, Puerto Rico USA 00936-5067

Corresponding Author

*Phone: 787-292-9820, fax: 787-522-2150; email: eduardo.nicolau@upr.edu

KEYWORDS zwitterion, polymer, PCBMA, TFC, selective layer, DSC, TGA, XPS

Abstract

Zwitterionic polymers have proven to be a promising non-fouling material that can be applied in the design of selective layers of thin film composite (TFC) membranes. Extending the permeability and usage of TFC membranes have attracted increasing interest in membrane-based desalination processes since water-flux reduction associated with biofouling persist nowadays as a common challenge. By virtue of its strong hydration, this polymer category is very useful to counteract biofouling in marine and biomedical systems, but the benefits from their application in membrane technology are still emerging. The efficacy of the non-fouling property as a function of the polymer's molecular weight remains unknown. In pursuit of that vision, this study fosters new scientific insights via probing different molecular weights of poly(carboxybetain methacrylate) (PCBMA) coated on the surface as a selective layer for the prepared TFC membranes. The coated zwitterionic membranes (zM) exhibited excellent performance to prevent water flux decay in a bench scale forward osmosis system. The prepared zM membranes revealed enhanced hydrophilic properties and retained its operational water-flux when compared to the control. Our results suggest that using an intermediate size molecular weight (PCBMA M_n 50,000) will result in the best operational performance. The intermediate size resulted in the lowest flux decline rate (R_t) of 0.01±0.001 (zM-50) when compared to the unmodified control membrane 0.56 ± 0.071 (M0) after using a model BSA foulant solution. Furthermore, all coated membranes exhibited similar trends in the observed reverse salt flux profiles as well. The constructed zM membranes will serve as a model to develop further selective layers in the construction of TFC membranes.

Graphical abstract

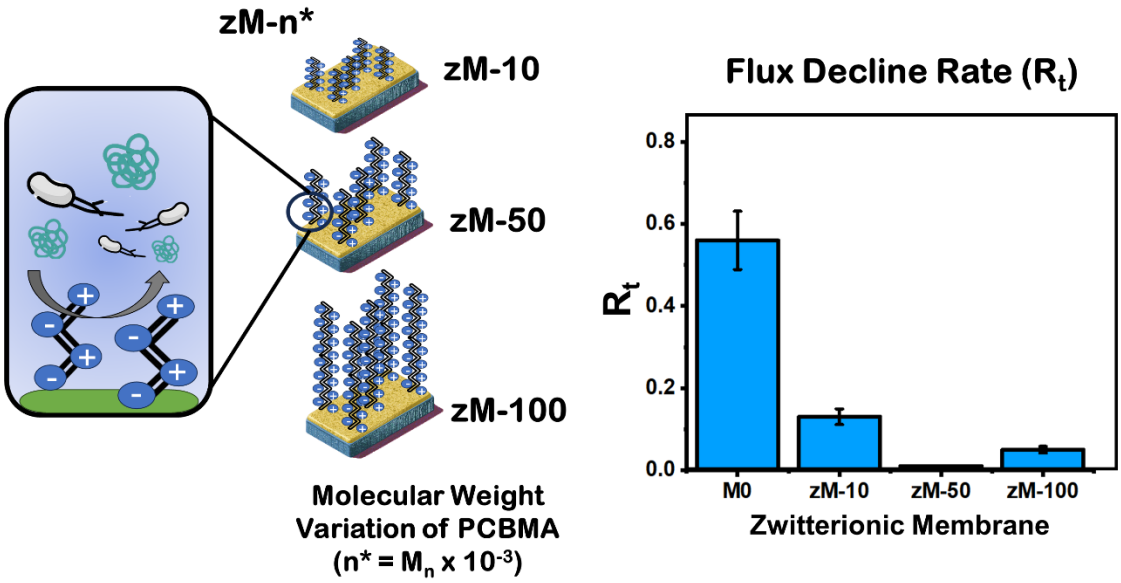

1. Introduction

The design of zwitterion-based selective layers of thin-film composite (TFC) membranes is rapidly capturing the attention in desalination strategies as a way to gain biofouling control and thus improve the overall filtration strategy. Selective layers have been independently optimized to achieve target filtration functions using different zwitterion chemistries over recent years to tailor the interfacial morphology and wettability of TFC membranes.[1-3] However, little attention has been given to the profound effect of polymers' molecular weights on the properties and performance of such selective layers.

The adhesion of organic matter tends to result in biofouling which becomes detrimental in keeping up operational efficiency in a treatment facility. In desalination treatment, operative expenses might increase up to an additional 50% due to biofouling difficulties which shortens membranes life.[4] In this context, environmentally friendly polymer zwitterions[5-7] are known to effectively counteract both bacterial and nonspecific protein adsorption that ultimately promotes biofouling at the surface of different materials.[3, 8] In general, previous works have shown that devices made from hydrophobic polymers are more prone to the accumulation of proteins and bacteria on their surfaces when compared to their hydrophilic counterparts.[9, 10] Despite, numerous TFC membranes having applied hydrophobic macromolecules to prevent the accretion of organic matter, the unconformity about membrane's efficacy persists. Conversely, the application of zwitterionic polymers is emerging as an alternate new class of material to tackle this challenge. This polymer category may swell when in water which eventually acts as a conditioning layer at the interface to prevent the initial adhesion of organic matter thus minimizing the interactions of fouling organisms at the surface.

In this context, polyzwitterions have acquired significant attention as superhydrophilic polymers by virtue of their strong fouling resistance. Indeed, diverse polymer-structure relationships will result in different material behaviors. The molecular weight (MW) of polymers intrinsically affects the properties of the final product that will be made from it. In general, some of these affected properties of the material include mechanical, thermal, morphological, optical, electrical, solubility, and durability.[11] In the field of water desalination, crafting selective layers by using specific polymeric characteristics such as molecular weight would tremendously help in tuning the target functionalities of its design. Previous molecular dynamics (MD) studies have established that the antifouling behavior of the polymer brushes is enhanced by increasing the grafting density.[12, 13]

Interest has arisen in using zwitterions polymers to dictate antifouling properties in the construction of forward osmosis (FO) thin-film composite (TFC) membranes. Notably, recent works have made strides towards "grafting-from" zwitterion molecules to craft the selective layer. Despite the extensively studied "graft-from" approach (i.e. atom transfer radical polymerization also known as ATRP)[1, 14-16] to anchor monomers of zwitterions might achieve controlled thickness[17] with predictable size, they do not provide the feasibility to accurately measure the actual average molecular weight and polydispersity (PDI) of the grafted zwitterionic polymer. A recent study proposed the relationship between the inhibition of nonspecific protein adsorption via the application of different spacer lengths of a carboxybetaine copolymer that might translate into different molecular weights of the polymer.[18] However, the study intended to promote the sensitivity of sensor devices but did not address the effect on TFC membrane performance. Another recent work studied the effect upon varying the concentration of the zwitterionic polymer on the FO performance using a constant MW.[19]

While recent experimental studies have proven the efficacy of the antifouling properties of different zwitterion chemistries[12, 13] on the interfacial layer, there's no information regarding the effect of varying the molecular weight of the polymer against the performance of FO TFC membranes along with its biofouling resistance. The lack of experimentation details at the molecular level makes it difficult to further design zwitterionic selective layers. Herein, this study connects the influence of the average polymer molecular weight to the performance by using a model zwitterion polymer, namely Poly (carboxybetaine methacrylate). The experiment studied the membrane water transport and fouling resistance properties when applied to a bench scale forward osmosis setting.

Poly(carboxybetaine methacrylate) also known as PCBMA is a zwitterionic polymer that has been widely studied and applied as an interfacial material in membrane based separation processes and biomedical applications.[20] Its intrinsic hydrophilic properties had proven excellent resistance in preventing nonspecific protein adsorption leading to fouling.[3, 21] Carboxybetaine was selected because it has been shown to have greater interaction in binding with water molecules (stronger and longer) when compared to other common zwitterions.[22] Moreover, previous studies have reported various applications of the material in different areas such as biomedical applications[23, 24], sensor developing[25, 26], and membrane separation technologies.[27-29] However, this resistance feature has not been explored as a function of the polymer molecular weight. This study incorporated different molecular weights of PCBMA (Table 1) to prepare the active layer of different thin-film composite (TFC) membranes and thus investigate their fouling-resistance and desalination properties using a forward osmosis setting.

Moreover, different works have reported the unique and interesting feature of salt-responsiveness for zwitterionic polymers[21]. When in salt solution, the zwitterionic polymer chains display a stretched conformation as opposed to a collapsed state when in water.[28, 30]

Table 1. Summary of the different PCBMA molecular weights applied

Membrane ID (zM-n)	Polymer ID	M_n	M_w	M_w/M_n
zM-10	PCBMA(10K)	10,000	18,000	1.80
zM-50	PCBMA(50K)	50,000	51,000	1.02
zM-100	PCBMA(100K)	98,000	134,000	1.38

The growing interest of zwitterionic polymers applications has led to different grafting methodologies. Grafting-from and grafting-to methods have been employed to coat the surface of materials by using common zwitterionic moieties such as carboxybetaine, sulfobetaine, phosphatidylcholine, and phosphobetaine.[8, 27, 31, 32] In general, zwitterionic polymers are known as "inner salts" and contain both positive and negative charged units within the polymeric structure that results in a neutral molecule. The hydrophilic layering will enable a high content of water molecules solvation at the interface that will function as a natural repellent to the organic matter, thus also inhibiting its attachment to the surface.

A common problem encountered with materials used for membrane-based separation processes is their water-flux reduction associated with biofouling due to surface microorganism attachment. Moreover, this work also aims to investigate the non-biofouling (NB) features of PCBMA under a fouling environment. The data from this study will serve as a model to further develop and design future zwitterionic selective layers applicable to TFC membranes.

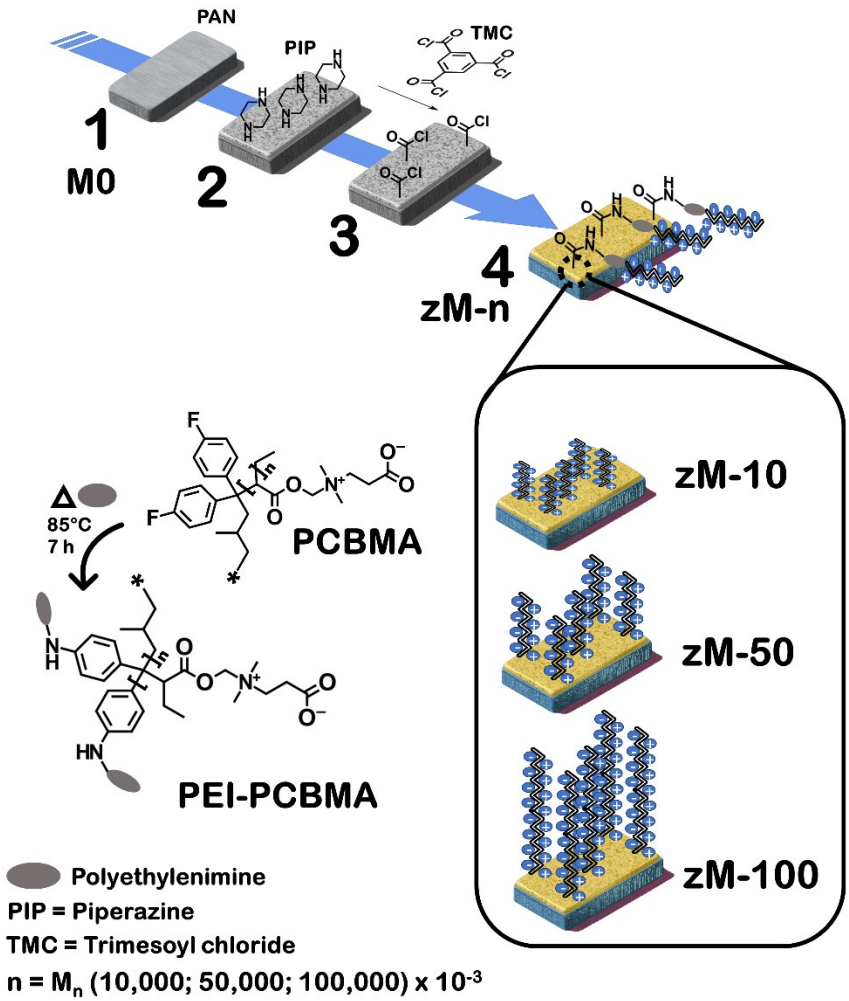

Figure 1. Illustration of the construction steps for the zwitterionic thin-film composite membrane (zM-n) and composition of each layer along the process.

2. Materials and Methods:

2.1 Materials. Polyacrylonitrile (PAN, Mw ~ 150,000), polyethyleneimine branched (PEI, Mw ~ 25,000), sodium chloride (NaCl, ACS reagent > 99%), piperazine (PIP, 99.5%), 1,3,5-benzene tricarbonyl trichloride (TMC, 98%), n-hexane (97%, anhydrous), and dimethyl sulfoxide (purity = 99.5%) were used as received from Sigma-Aldrich (Saint Louis, USA).

Zwitterionic polymer, poly(carboxybetaine methacrylate) were sourced from Polymer Source (Montreal, Quebec, Canada) custom synthesized at different molecular weights (M_n:10,000, 50,000, and 98,000). Bovine serum albumim labelled with CF 594 (BSA-CF594) was purchased from Biotium Inc. (Fremont, CA). *Pseudomona Aeruginosa* (PA01) with a plasmid expressing a green fluorescent protein (GFP) was purchased from ATCC (ATCC, 10145GFP). Nutrient broth (BD 234000) and ampicillin were purchased from Bio-Rad laboratories (Hercules, CA, USA). A polyester (PE) woven mesh (105 μm, 52% open area) was purchased from Elko Filtering Co. Nano pure water (18.2 MΩ-cm^2, Milli Q Direct 16) was used during all experiments and cleanings.

2.2 Fabrication of the support and zwitterion coated thin-film composite (zTFC) membranes. Initially, we prepared the support membrane (control membrane labeled as M0) using a casting solution of 12.5% (w/v) polyacrylonitrile (PAN) in DMSO dope with 2% (w/v) LiCl, as reported elsewhere with some adjustments.[31, 33] Briefly, the dope solution was left stirring overnight at room temperature. Then, a polyester woven mesh was fixed over a clean glass surface to add mechanical strength. Thereafter, the PAN solution was blade casted at 120 μm thickness over the polyester mesh and subjected to the nonsolvent induced phase separation (NIPS) process. Then, the support membrane (M0) was left for at least 30 minutes in the water bath and rinsed with nano pure water prior to further modifications to remove any residual solvent.

Afterward, a polymeric solution of PEI-PCBMA was synthesized similar to previous works[34, 35] using the corresponding molecular weight (M_n:10,000, 50,000 or 98,000) of PCBMA into an aqueous 2% (w/v) PEI solution. The solution was stirred and heated in an oil bath for 7 hours at a temperature of 85°C. The resultant reaction product was purified by using a 5 kDa

dialysis tube for at least 72 hours. Subsequently, the solution was frozen at -20°C prior lyophilization.

Thereafter, the zwitterion coated membranes were fabricated via a conventional interfacial polymerization (IP) method as shown in Figure 1.[27, 36-38] Briefly, a 0.3 wt % PIP aqueous solution was poured over the membrane surface for 5 min[30]. A less dense polyamide layer is usually formed when using a PIP/TMC system when compared to MPD/TMC because an amine monomer such as PIP usually produces a thin semi-aromatic layer.[39] The excess of PIP solution was removed from the membrane surface using a rubber roller and then a TMC organic solution in n-hexane (0.15 wt %) was quickly poured on top for 1 min to produce a polyamide film. The residual -COOCl groups[37, 38] at the surface of the polyamide layer were used to react with aqueous PEI-PCBMA solution (1 wt %) of each molecular weight for at least 5 minutes. The final membranes were annealed at 70°C in an oven for 5 minutes. This procedure was repeated for a total of three membrane replicates. The prepared membranes were stored at refrigeration temperature of 4°C – 8°C. The prepared zwitterion coated TFC membranes were washed and stored in nano pure water until further use. The thin film composite membranes were denoted as zTFC-n, where n represents the abbreviated numbering of the molecular weight (labeled as zM-10, zM-50, and zM-100 indicating the corresponding molecular weights of M_n:10,000; 50,000; and 98,000, respectively). For example, zTFC-10 membrane was prepared using PCBMA with a molecular weight of M_n 10,000.

2.3 Characterization Techniques. The physico-chemical characteristics of the constructed zwitterionic membranes of different molecular weights were verified to confirm the deposition of the polymer and expected functionalization. The employed characterization techniques are described below.

2.3.1 Fourier-Transform Infrared Attenuated Total Reflectance (FTIR - ATR) Spectroscopy

The functional groups for the used materials were characterized by means of Fourier-transform infrared (FTIR) spectroscopy (Bruker Tensor 27 attenuated total reflectance (ATR) spectrometer, Billerica, MA, USA). Infrared spectra were collected in the range from 400 to 4000 cm^{-1}4 cm^{-1}resolution, and accumulation of 64 scans.

2.3.2 X-ray Photoelectron Spectroscopy (XPS). XPS examination was completed using an ultrahigh vacuum (UHV) system (~2×10^{-9} Torr) equipped with a hemispherical electron energy analyzer (SPECS, PHOIBOS 100, MCD-5) and twin anode X-ray source (SPECS, XR50). A non monochromatized Al Kα ($h\nu$ = 1486.6 eV) X-ray source at an accelerating voltage of 15 kV, and 20 mA current was used for the analysis. The angle between the analyzer and X-ray source is 45 degree and photoelectrons were collected along the sample surface normal. The XPS analysis regions measured were 280−295 eV for C 1s, 525−540 eV for O 1s, 395−410 eV for N 1s. To measure each individual region, we employed a step size of 0.05 eV and scan number of 15. Charge correction for the data was done by adjusting the adventitious carbon C 1s binding energy located at 284.6 eV. XPS data was analyzed using Casa XPS and Origin softwares.

2.3.3 Differential scanning calorimetry (DSC). The thermal responses of the modified polymers were studied by DSC using a PerkinElmer Diamond DSC. Samples with masses of approximately 15 mg were dispensed in aluminum crucibles with pierced lids and helium was applied as purge gas. Thermograms were obtained in two cycles between -40°C and 100 °C with heating at 10°C min^{-1} and cooling at 40 °C min^{-1}. Only the curves for the second heating cycle were considered to eliminate thermal history artifacts. The DSC thermograms were inspected for glass transition (T_g) or melting temperatures.

2.3.4 Thermogravimetry analysis (TGA). Polymers (before and after the conjugation) were evaluated using TGA (PerkinElmer Diamond TG/DTA). The measurements were performed by heating approximately 10 mg of solid polymer under argon gas purging from room temperature to 550°C at a rate of 10 °C min^{-1}.

2.3.5 Scanning Electron Microscopy (SEM)

The morphology of the membranes was inspected using scanning electron microscopy (SEM/SEI, JEOL 6480LV) with an electron beam energy of 20.0 kV accelerating voltage in the secondary electron imaging (SEI) mode. Pelco ® Auto Sputter Coater SC-7 (Ted Pella Inc., Redding, CA) was used to coat the samples using platinum at a current of 40 mA.

2.3.6 Atomic Force Microscopy (AFM)

The surface roughness of the top layer was inspected using a FastScan ScanAsyst atomic force microscope (AFM Park NX-20) in noncontact mode (NC) at the Center for Functional Nanomaterials in Brookhaven National Laboratory. The ScanAsyst-Air Bruker tips used have a silicon tip on a nitride lever (Bruker AFM Probes, Camarillo, CA) with a spring constant of 0.4 N/m. Measurements were taken in air with square sections of 2 μm x 2 μm, an aspect ratio of 1, scan angle of 0◦, and no X or Y offset. Thereafter, analysis of the images and the root-mean-square surface roughness were completed using XEI software. Three arbitrary locations of the samples were used to measure the root-mean-squared roughness (R_q) and the average roughness (R_a).

2.3.7 Surface Contact Angle and Underwater Contact Angle Characterizations

To examine the hydrophilicity of the prepared membranes, contact angle was conducted using a Krüss drop shape analyzer DSA25S (Krüss Optronic, Hamburg, Germany) at

ambient conditions. The contact angle of the deposited zwitterion coated layers were measured using the sessile drop experiment (water-in-air). Membranes coupons size of 2.25 cm^2 area, a 25-gauge flat needle, and a water droplet of 4.50 µL DI water were used during the measurements. Then, images of the drop at the air/polymer interface were recorded timewise up to 120 seconds (using intervals of 0.5 seconds). Contact angle data were analyzed in real time using Advance software (version 1.8). Uncoated PAN membrane (M0) was also measured as the control. Three sessile drop measurements were made on each membrane and the average values were reported.

Thereafter, captive bubble contact angles (underwater contact angle) images were recorded using a sessile method involving a digital microscope equipped with a custom-made cell filled with nano pure water (ρ >18.2 MΩ·cm), and U-shape micro syringe, and immiscible fluids (oil and air) as reported elsewhere.[30, 40] A 'J'-hook needle was used to dispense an air bubble 4 µL of mineral oil or air bubble from beneath the membrane sample. The experiments were made at room temperature (22°C) and the cell was placed on a granite base to minimize any vibration effect.[41] The images were captured using a digital microscope (Dino-Lite Pro AM4113T) with a high quality image sensor through transparent glass windows. The setup was placed on a stable table.[42] The resulting contact angle (oil/air) at the polymer-water interface was digitally measured using NIH ImageJ program with a contact angle plugin function as published elsewhere.[43, 44] The average of three measurements of each contact angle on each individual surface is reported. Hereafter, to understand the modulation of the surface energy (estimation of the Interfacial Surface Energy), we employed the derivations of the equations as reported elsewhere.[21]In brief, the measured underwater contact angles of both immiscible liquids (oil/air) were used in the

combined equation form of Young's equation and Wu's estimate of interfacial tension[45] to calculate the Interfacial Energy (IFE) at the zwitterion/water interface.

2.3.8 Surface Zeta Potential

The surface charge of the zwitterion-coated membranes was measured with an Anton Paar SurPASS 3 using an adjustable gap cell. Membrane coupons sizes 20 mm × 10 mm were used. The system was initially rinsed with DI water. A background electrolyte solution consisting of 0.1 mM potassium chloride was employed.[46]The pH was adjusted to values ranging from 3 to 10 using aliquots of 0.1 M hydrochloric acid and 0.1 M potassium hydroxide. All measurements were collected in triplicate at each pH.

2.4 Forward osmosis (FO) membrane performance. The separation performance of the zwitterion coated membranes were evaluated on a bench-scale forward osmosis (FO) system. The forward osmosis (FO) cell used during all experiments did not promote any turbulence in the feed or draw solution sides. A membrane coupon with an exposed area of 4.25 cm^2 was used for all FO experiments. The membranes were evaluated under the AL-FS (active layer facing the feed solution) operational mode at 22.0 ± 0.5°C and 0.2 L/min cross-flow rate. The water transport was recorded using a digital balance, and the solute reverse flux was monitored by using a conductivity meter (Cond 3310, WTW, Germany). The osmotic performance was assessed after one hour of operating the system at room temperature and atmospheric pressure. Nanopure water (18.2 MΩ-cm^2) was used on the feed side and a 0.5 M sodium chloride (NaCl) solution was used at the draw side during all experiments. Thereafter, a 100 ppm BSA foulant solution was also used to investigate the antifouling behavior of membranes in a FO setup. Initially, the membranes were tested against nanopure water for 60 minutes to assay the water transport property, and then the feed solution was replaced with the BSA foulant solution to

conduct the fouling test for an additional 60 min. Subsequently, water cleaning was conducted three times before repeating the experiment. The collected permeated water from the feed to the draw side was calculated by using the following equation: $J_w = \Delta V /(A_m \times t)$, where the V corresponds to the difference of the final and initial recorded volume (L), A_m corresponds to the area of the membrane (m^2), t corresponds to the experiment running time (h), and J_w is the water flux in LMH (L m^{-2} h^{-1}). Similarly, the reverse salt flux (J_s) in mMH (mol m^{-2} h^{-1}) was calculated by using the equation: $J_s = (\Delta CV) / (A_m \times t)$, where ΔCV corresponds to the difference between initial and final salt concentrations times the feed side volume. Then, the flux decline ratio (R_t) and the flux recovery ratio (FRR) were calculated as follow: $R_t = (J_o - J_s)/J_o$ and $FRR = (J_r/J_o)x100$, where J_o correspond to the initial flux, J_s to the steady water flux using fouling conditions, and J_r to the recovered water flux after washing.[47] Three replicates were performed for each membrane. Data indicates the mean +/- standard deviation, n=9.

2.5 Protein (BSA) adsorption experiment. The static fouling resistance attribute of the hydrophilic membranes was tested by employing a fluorescence protein adsorption experiment. Bovine serum albumin with fluorescent dye conjugates (BSA-CF594) was used as a model protein to assess the extent of protein adsorption over the deposited zwitterion coating as a function of the polymer molecular weight. Membrane coupons with an effective area of 2.25 cm^2 were initially submerged in nano pure water for at least 24 hours. Then, the protein fouling experiment began by removing the excess water of the coupons and immersing the membranes in a 50 ppm BSA-CF594 solution for 3 hours of contact time. After completing the fouling test, the membrane coupons were removed from the BSA solution and rinsed three times with PBS before mounting them in a glass slide. Thereafter, the photographs of representative fields of view were taken with the DS-Qi2 digital camera attached to the

Fluorescence microscope (Nikon Eclipse, Ni-U) at a wavelength of 593 nm (exposure time = 3.3 ms; analog gain=11.4) and further analyzed with Nikon NIS-Elements (Basic Research Version 5.30.03) software. Recorded images have a resolution of 1068 x1068 (14 bit). The fluorescent intensity measurements across the images were performed by subtracting the intensity of a background image from the intensity of the entire region of interest (ROI) across the membrane.

2.6 Bacteria resistance performance. The bacterial resistance capability on the membrane's surface was evaluated by the extent of adhered cells after 3 hours of contact with a bacterial culture. *Pseudomonas aeruginosa* PA01 with a green fluorescent protein reporter gene was used as a model organism because of its ability to thrive in highly saline environments. The substratum coverage was determined by the mean fluorescence intensity of the coupons. We used a Nikon A1R laser scanning confocal system at a magnification of 1000x to carry out these observations.

The bacterial adhesion on the membrane's experiments were adapted from elsewhere with some modifications. In brief, a bacterial suspension with a cell concentration of 10^{-6} to 10^{-7} CFU/mL was prepared in 0.9% NaCl. Three replicas of each membrane using a coupon size of 2.25 cm^2 were individually immersed in a well of a 9-well plate previously filled with 2 mL of the standardized bacterial suspension (top surface of the coupon exposed to the suspension). The samples were incubated at 37°C and shaken at 100 rpm for 3 hours. Next the bacterial suspensions were removed from each well and the membrane coupons were washed three times with 2 mL 0.9% NaCl solution. Then, bacteria attached to the membrane were fixed using a 4% PFA solution. Afterwards, the mounting media was added, the images of the coupons were acquired by a Nikon A1R Laser confocal system using a 100x/1.45 oil immersion objective.

To collect the images, cells were excited at 488 nm and a band pass filter 505-550 nm was used to visualize GFP. At least three images of each biological triplicate were collected. The acquired images were analyzed using NIS-Elements AR analysis Version 5.2 to determine the mean fluorescence intensity of each coupon. To conduct the statistical analysis, a software GraphPad Prism 7.0 was used to analyze the collected data. An unpaired t test was used to determine statistical significance, where***$p < 0.001$ and*$p < 0.033$. Data are shown as mean ± standard deviation.

3. Results and Discussion:

Our aim in this work was to investigate the effect of varying the molecular weight of PCBMA on the active layer of a thin film composite (TFC) membrane to study the biofouling resistance of the material and thus improve the operational water flux against biofoulants during desalination. It might be thought of a higher molecular weight of the zwitterion polymer will contain a denser brush composition thus providing a tighter layer of solvation that could better prevent adhesions of organic matter at the water-polymer interface of the membrane. In the context of the underneath support layer, polyacrylonitrile (PAN) based materials had been widely studied for different applications including biomedical applications, process filtrations, and water treatment membranes[9, 48, 49] PAN is a common inexpensive polymer that is relatively more hydrophilic compared to other polymeric materials such as Polysulfone (PSF), Polyethersulfone (PES), and Polyvinylidene difluoride (PVDF).[47]. However, the selective layer has a significant role in the membrane separation process as it acts as the initial interfacial barrier against contaminants. It has been widely studied how the life span of membranes is shortened under biofouling conditions.[21] The initial organic matter adsorption to the surface of the material has an irreversible effect that affects the membrane performance within a treatment operation. Therefore, researchers have been

questing for different physical and chemical modifications of material's interface that counteract this detrimental effect and thus extend the membrane operation. The introduction of zwitterionic polymers as part of the selective layer of TFC membranes has been recently studied by multiples groups[23, 50] which lead us to the question how the molecular weight could tune the membrane hydrophilicity and its biofouling resistance properties.

In this work, the surface of a PAN based membrane was modified with PCBMA by employing a fast second interfacial polymerization (SIP) method[12, 41] instead of growing polymer brushes on the surface. Interfacial polymerization is considered an efficient and fast preparation method to fabricate thin-film composite (TFC) membranes.[51] Briefly, the PAN support membrane is subjected to interfacial polymerization by initially forming a polyamide layer upon contact of a PIP solution followed by a TMC solution. Thereafter, the residual amounts of -OCl groups are used to attach PEI-PCBMA of different molecular weights. By varying only the molecular weight variable in the preparation of the selective layer, the interfacial properties also change as discussed in the following sections.

X-ray photoelectron spectroscopy results. The individual layers of the zwitterionic membranes were chemically characterized on the surface to confirm material deposition after the preparation process. X-ray photoelectron spectroscopy (XPS) was employed to inspect the elemental compositions and chemical states (C1s, O1s, N1s) of the deposited zwitterion layer. Figure 2a shows the results for the surface examination of the constructed membranes by varying the molecular weight. The survey scan spectra for the M0 (PAN) and polyamide membranes are included in the supporting information, Figure S1. The general XPS spectrum indicates the existence of the expected elemental composition namely carbon, nitrogen, and oxygen in all three

modified membranes. Both bands for N1s peak at 400.0 eV and O1S peak at 531 eV confirm the successful deposition of the PCBMA layer on the top of the membrane's surface.

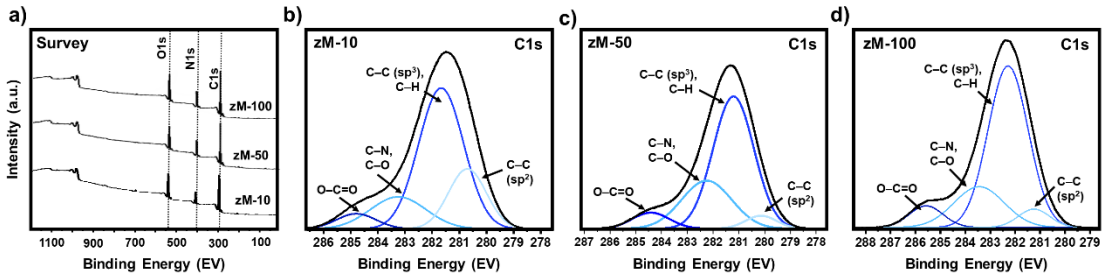

Figure 2 (a-d). X-ray photoelectron spectroscopy (XPS) results. a) survey scan and b – d) C1s high resolution spectra for the three different molecular weight of the zwitterion coated membranes.

Moreover, the quantification of atomic composition of each sample was estimated for the survey data and summarized in Table 2. The increase in atomic percentage of the relative Nitrogen confirms the increase of PCBMA molecular weight.

Table 2. Relative atomic composition of the different zwitterion coating molecular weights.

	Relative Atomic Percentage (%)		
Sample ID	**C (%)**	**N (%)**	**O (%)**
zM-10	70.0	10.9	19.1
zM-50	67.4	13.7	18.9
zM-100	72.6	18.8	8.7

In addition to the survey scan, it was of interest to inspect the C1s binding energy of each molecular weight of the zwitterionic polymer. To this end, a C1s high-resolution deconvolution spectra was completed for all samples. The de-convoluted C1s spectrum for zM-10, zM-50, and zM-100

samples (Figure 2, b - d) were completed using four dominant Gaussian–Lorentzian peaks at different resolved binding energies (BE). Table S1 (supporting information) summarizes all the binding energies and compositions obtained for this analysis. It is worth noting the signals near 286 eV (C – N / C – O) and 288 eV (C=O) are related to the zwitterion polymer coating. These binding energies are associated to the amine bonds corresponding to the amino group as well as to the carboxylic bonds present in the zwitterion moiety. We confirmed an increasing trend for the area percentage of the C – N / C – O band for the samples with higher molecular weights. The area percentages of the bands were 16.2% (zM-10), 22.2%(zM-50), and 47.4% (zM-100). Therefore, our results for the surface characterization with XPS confirm that the membranes were successfully constructed with the different molecular weights of PCBMA adlayer.

In an effort to conduct a holistic characterization of the material, infrared spectroscopy was also employed in order to inspect the functional groups at the surface.

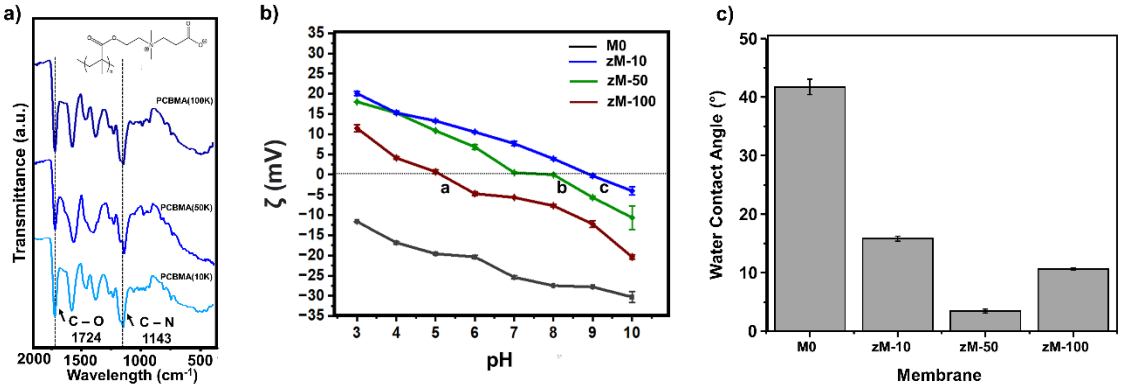

Figure 3 (a–c). Physico-chemical characterization of the membranes surface. a) infrared spectroscopy, b) surface zeta potential (ζ), and c) contact angle.

As shown in Figure 3a, the absorption peaks corresponding to the C=O stretching vibrations in the ester group of the grafted PCBMA at 1724 cm^{-1} and the C-N bending attributed to the amine group

at 1143 cm^{-1} were identified.[52] Both XPS and infrared data confirm the successful grafting of PCBMA on the membranes' surface.

Surface Zeta potential (ζ) results. Furthermore, the membrane's surface charge was also inspected using surface Zeta potential (ζ). The results for streaming surface potential profiles as a function pH is shown in Figure 3a. The monotonically reduction in zeta potential values with increasing pH for zM-10, zM-50, and zM-100, as opposed to the negatively charged trend of M0, confirms the successful layer deposition as well. The control M0 trending is in agreement with previous works found in the literature.[53, 54] Compared to the control, the zwitterion coated membranes revealed its IEP at pH 8 (zM-10), 9 (zM-50), and 5 (zM-100). It is interesting to observe that the intermediate molecular weight used in zM-50 revealed the most neutral surface charge near neutral pH values. Moreover, at neutral pH 7 the membrane with the lowest zwitterion MW (zM-10) revealed a positive surface charge while the highest employed MW (zM-100) was predominantly negative. This property could help tune the membrane surface charge as a function of the molecular weight and this can further help to mitigate the adhesion of organic matter due to columbic interactions. The separation distance of the zwitterionic moieties is affected by the molecular weight size, despite the zwitterion unit containing an equal amount of cationic and anionic groups. The higher the molecular weight, the denser brushes distribution, and thus the shorter the separation distance. A previous study reported that such zwitterion groups are able to undertake electrostatic interactions between their own moieties with the capacity to internally self-associate in charge combination.[32] The charge density of the anionic carboxyl group is more negatively richer when compared to the low positive charge density of the quaternary amine group.[32] It is expected that at the higher molecular weight of the zwitterion polymer, the surface charge will be richer in negative charges due to the more presence of carboxyl groups. Therefore,

the protons available in the acid medium can interact with the anionic group thus resulting in a positive surface charge at acid pH ranges. In the other hand, a predominant negative charge is expected at higher pH values due to the absence of available protons to neutralize the denser charge of the carboxyl groups, which explains the zM-100 trend in Figure 3b. The zwitterion coated membranes did not present a neutral surface charge at neutral pH 7 as expected, ascribing to the following reason. The positively charged quaternary amine groups of both the zwitterion and BPEI linker predominates the overall charge density at the surface of the membrane when compared to the negative charge contribution of the carboxyl groups. Consequently, the positive charges predominate at less dense polymer brushes used at lower molecular weights which shift the IEP to higher pH values. Therefore, we determine a successful deposition of PEI-PCBMA at the membrane interface at the different molecular weights.

Contact angle results. To evaluate the effect of increasing the molecular weight of PCBMA on the hydrophilicity of the membranes, water contact angle (WCA) was employed using the sessile drop method at ambient temperature. A material with a smaller water contact angle will indicate a more hydrophilic surface. As shown in Figure 3c, zwitterion coated membrane resulted in much less water contact angles when compared to the unmodified support PAN membrane (M0). The water contact angle of the prepared membranes significantly decreased from 41° (M0) to 15° (zM-10), 3.4° (zM-50), and 10.1° (zM-100). Interestingly, the WCA for zM-50 revealed the smallest angle for the studied molecular weights. We hypothesized that this significant reduction in the angles can be attributed to the large number of amines groups grafted at the surface with PCBMA increase the hydrophilicity holistically. The observed results confirm our strategy to increase the affinity of water molecules to the membrane surface by introducing zwitterion based functional groups that display strong hydrophilicity properties at the interface of the designed material.

Furthermore, we also verified the underwater contact angle (oil-water/captive air) of the membranes. Underwater contact angle measurements provide useful information about how the zwitterion functional groups interact when in a complete water environment. In this experiment, the angles were measured using two different probing bubbles. Mineral oil and air were used to make the bubble at the membrane's solid surface immersed inside a water tank. The images were captured using a digital microscope for each probing substance. Thereafter, the resulting angles were estimated using the NIH ImageJ open software.[46]

Table 3. Summary of underwater contact angle for the support and zwitterionic membranes of different molecular weights

Membrane	Underwater Contact Angle, oil bubble (ϕ°)	Underwater Contact Angle, air bubble (θ°)	Interfacial Energy (IFE)
M0	120 ± 1.7	102.4 ± 1.8	1558.0
zM-10	127.3 ± 1.3	140.1 ± 0.2	1509.3
zM-50	148.8 ± 0.9	150.1 ± 0.3	1273.2
zM-100	136.7 ± 0.1	146.6 ± 0.2	1545.4

In this method, a larger internal angle of the probing bubble indicates an increase in the surface hydrophilicity. Likewise, more hydrophilic material corresponds to an increase of membrane wettability. A summary of the underwater contact angles is included below in Table 3.

The results obtained revealed a marked increase in the inner contact angles when measured in underwater conditions. The angles values were used to calculate an estimation of the interfacial energy (IFE) at the polymer-water interface using equations[21] and thus compare the result for the different molecular weights.

Where,

$$IFE = \gamma_{pa}^{Tot} + \gamma_{WA} - 4\frac{\gamma_{pa}^{d}\gamma_{wa}^{d}}{\gamma_{pa}^{d} + \gamma_{wa}^{d}} - 4\frac{\gamma_{pa}^{p}\gamma_{wa}^{p}}{\gamma_{pa}^{p} + \gamma_{pa}^{p}} \quad (1.1)$$

$$\gamma_{pa}^{p} = \frac{\gamma_{wa}^{p}\left(\gamma_{wa}(1 + cos\theta) - 4\frac{\gamma_{pa}^{d}\gamma_{wa}^{d}}{\gamma_{pa}^{d} + \gamma_{wa}^{d}}\right)}{4\gamma_{wa}^{p} + 4\frac{\gamma_{pa}^{d}\gamma_{wa}^{d}}{\gamma_{pa}^{d} + \gamma_{wa}^{d}} - \gamma_{wa}(1 + cos\theta)} \quad (1.2)$$

$$\gamma_{pa}^{d} = \frac{\gamma_{OA}(\gamma_{wa}cos\theta - \gamma_{WO}cos\varphi) + \gamma_{OA}^{2}}{\gamma_{WO}cos\varphi - \gamma_{wa}cos\theta + 3\gamma_{OA}} \quad (1.3)$$

The lower the IFE, the better anti-fouling properties should be observed at the interfacial layer. The estimation for the IFE revealed a higher wettability of the membrane after the zwitterionic polymer deposition. In fact, zM-50 obtained the lowest IFE value for all three molecular weights, suggesting better anti-fouling resistance for this molecular weight. The obtained results confirm the effectiveness of the method of deposition used.

Scanning electron microscopy (SEM) and atomic force microscopy (AFM) results. SEM and AFM were employed to characterize the surface morphologies of the different TFC membranes before and after using the zwitterion coating. Despite no visible organized pores were detected in the selective PCBMA layer of the SEM micrographs (Front view row in Figure 4) at the observed magnification (x45,000), there is a subtle change in the physical aspect. The grainy surface structure of the control membrane M0 was further smoothened after attaching the zwitterionic layer in zM-10, zM-50, and zM-100. Thereafter, the surface characteristics were scanned at 2-micron scale using AFM technique (Figure 4). The support membrane revealed a nodular pattern at the top side (Figure 4, AFM micrographs), while the zwitterion coated are smoother with no visible pore or ridge-and-valley patterns thus revealing a dense deposition of the zwitterion coating

at the top layer. This was confirmed with the average roughness measurements (R_a) obtained by means of AFM (Figure 4). The R_a values obtained after the zwitterion coating were lower resulting in 6.0 nm (zM-10), 4.0 (zM-50), and 5.3 (zM-100) when compared to the control membrane M0 (7.2 nm). The cross-section SEM images revealed an initial finger like structure that predominates at M0 and then a thin layer is observed upon increasing the molecular weight (Figure 4, cross section). The thickness increase (Figure S2 and Table S2 of supporting information) also confirms the effectiveness of the deposition method. The backside micrographs showed the modified membranes kept the open pores similar to the unmodified membrane used as the control.

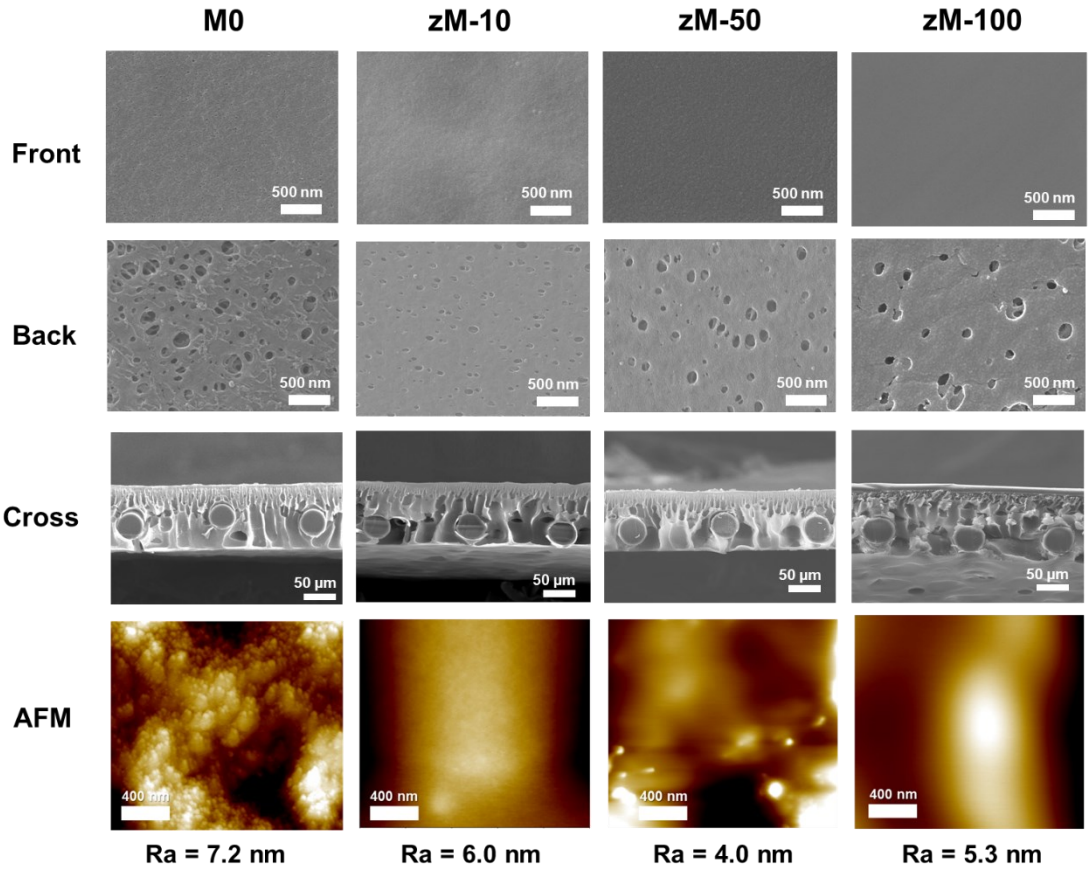

Figure 4. SEM and AFM micrographs of the unmodified (M0) and zwitterionic membranes for the different molecular weights (zM-10, zM-50, and zM-100).

The resulting images of the top layer revealed differences in average roughness as a function of the polymer molecular weight as mentioned earlier. The zwitterion coating notably improves the surface roughness of the top selective layer. A smoother top layer is expected to improve the biofouling resistance by reducing the potential ridges and valleys on the membrane surface that could promote foulant deposition.[47] The difference in surface morphology is mainly ascribed to the increase in the molecular weight of PCBMA were the impact of zwitterion attachment on surface morphologies was more prominent when using the mid-size molecular weight (zM-50). The effect of using mid-size polymer molecular weights also impacted on the hydrophilicity properties of the top selective layer as observed in Figure 3c in which lowest contact angles were also observed for the zM-50 membrane. Undoubtedly, the SEM and AFM results confirm the expected morphology of the membrane after the polymer zwitterion coating. Moreover, the aforementioned physical and chemical characterizations confirm the presence of the expected functional groups of interest regarding the PCBMA architecture that will impart the zwitterionic properties to the membrane performance.

Operational Performance of Zwitterionic Membranes

Water Transport Performance. The water (J_w) and reverse solute (J_s) fluxes were measured using a cross flow forward osmosis (FO) apparatus with the zwitterion coating (active layer) facing the feed side. To study the effect of varying the molecular weight on the selective layer, we initially conducted experiments using nano pure water (18.2 MΩ·cm) in the feed side to measure the water transport properties. Thereafter, we introduced a 100 ppm BSA solution in the feed side as a model protein foulant to conduct experiments. BSA was selected as a foulant protein model because most soils constituents found in water sources that act as membrane foulants usually exhibit an overall negative surface charge. A 0.5 M NaCl solution was used on the draw side. The detailed results of

J_w and J_s are shown in Table 4 and graphed results in Figure 5 (a – c). When tested against pristine water the obtained averages J_w for all zwitterion coated membranes slightly increased when compared to the unmodified control M0.

Table 4. Summary of the water transport properties for the different molecular weight's membrane

	Water			BSA	
Membrane	**J_w (LMH)**	**J_s (mMH)**	**J_s / J_w (mol/L)**	**J_w (LMH)**	**J_s (mMH)**
M0	7.6 ± 1.6	0.28 ± 0.06	0.037 ± 0.009	2.7 ± 1.2	0.40 ± 0.07
zM-10	8.8 ± 1.5	0.27 ± 0.09	0.031 ± 0.003	7.8 ± 1.4	0.26 ± 0.01
zM-50	10.5 ± 1.6	0.27 ± 0.08	0.026 ± 0.005	9.9 ± 1.5	0.23 ± 0.01
zM-100	8.7 ± 1.3	0.29 ± 0.06	0.033 ± 0.006	8.1 ± 1.3	0.27 ± 0.05

Certainly, the increase effect of J_w was not proportional to the increment of the molecular weights. Permeance governs the main mechanism for the transport of water molecules across the constructed zTFC membranes. Zwitterionic polymers greatly enhance water permeability by increasing the hydrophilicity of the membrane. Despite its overall neutral charge, zwitterionic polymers contain moieties of high charge densities which vary upon increasing their molecular weight that will eventually affect the water binding properties. Previous studies on PCBMA molecular simulations have revealed that the packing structure of a polymer brush is intrinsically related to the chain orientation, where longer pendant sidechains energetically preferred to adopt larger unit cells orientation.[22] Therefore, J_w is directly related to the effect of the electrostatic interactions of polymer brushes with the binding interaction to water molecules.

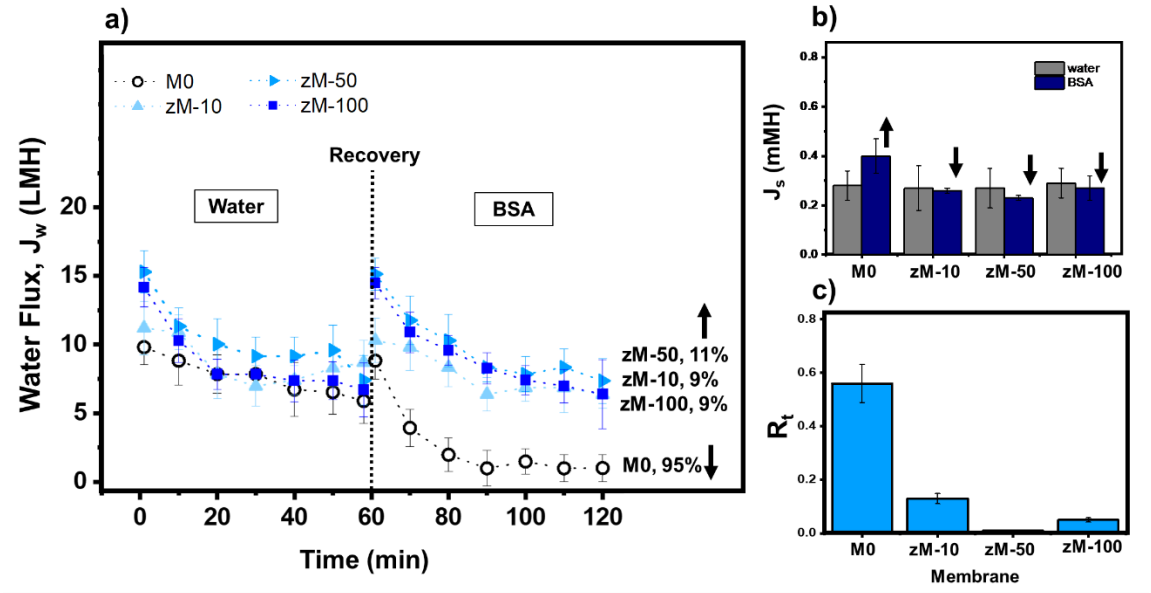

Figure 5. Water transport performance results of unmodified and zwitterion coated membranes. a) Water flux (J_w,) of the different molecular weight's membranes. Water flux results indicate J_w (LMH) and b) J_S (mMH) operated in FO mode with different feed side solutions. The experimental conditions as feed contaminant for FO runs included: nanopure water and 100 ppm BSA solution. All experiments used a draw side solution of 0.5 M NaCl. The membrane's performances were evaluated at room temperature for a run time of 60 minutes. Data indicates the mean +/- standard deviation, n=9. c) Calculated flux decline rate (R_t) for the different zwitterion coated membranes.

We hypothesized that the low molecular weight such as zM-10 might not bind enough number of water molecules strong enough to significantly increase its permeability due to a sparse packing density at the interface. On the other hand, at high molecular weights similar to zM-100 would also represent a weak water binding interaction. Presumably, the numerous numbers of brushes would be tightly packed at the selective layer thus zwitterion charges might interact with each other stronger rather than to water molecules. Additional computational simulation studies would be beneficial to elucidate the charges interactions as a function of incrementing PCBMA molecular weight. Our results revealed that the average size used to prepare zM-50 would translate in a membrane with the highest hydrophilicity as supported by the contact angle test (Figure 3c) showing the lowest angle of all prepared membranes. A greater hydrophilicity at this molecular

weight is achieved presumably because the hydrogen bonding between water and carboxylate group is facilitated at this polymer size which would enhance the chain distributions at the selective layer. Overall, the increased hydrophilicity along with the peculiarities of the resulting morphologies at the different molecular weights resulted in an enhanced water flux after the incorporation of PCBMA. Moreover, the stretching of the polymer brushes in presence of salt ions promotes tighter bonds of water molecules due to electrostatic interactions, hence producing a solvated selective layer with enhanced mass water transport (J_w) across the membrane.[55, 56] Furthermore, an additional experiment for zM-10 (supporting information, Figure S3) proved that the modified membrane retains stable after repeating the FO experiment 90 days of post storage conditions in deionized water at refrigerated temperature (2-8°C).

In terms of the reverse salt flux, our results show a similar J_s trend for all three zwitterionic coated membranes. The observed values of J_s for zM-10 (0.27 ± 0.09 mMH), zM-50 (0.27 ± 0.08 mMH), and zM-100 (0.29 ± 0.06 mMH) did not change notably when compared to the unmodified membrane M0 (0.28 ± 0.06 mMH). The experimental behavior suggests that increasing the PCBMA molecular weight on the selective layer has no direct reduction effect on the reverse salt flux when tested against nanopure water. It is hypothesized that the diffusion of salt ions from the draw side solution is influenced by migrating towards the feed side due to the presence of charged groups constituting the PCBMA chemical structure (Figure 1). Despite typical FO membranes normally rejects salt ions, previous works on thin films containing zwitterions had resulted in greater salt sorption when compared to uncharged polymers coatings.[57] In presence of charged moieties, small cations and anions will bound to the charged sites on the zwitterion. Similar effect had been observed in additional studies[2, 58] where an increase of water sorption at the zwitterionic layer results in higher salt permeability. Thereafter, the specific reverse salt flux J_s/J_w (Table 4)

was found to be slightly higher when compared to uncharged TFC membranes.[51, 59, 60] However, when compared to previous zwitterionic TFC membranes, J_s/J_w behaves similar as found in the literature.[2, 19]

Moving on to further fouling experiments, the average water flux J_w notably declined for the control membrane M0 from 7.6 LMH versus 2.7 LMH when using the simulant BSA foulant solution (Table 4). This represents nearly 95% of difference of water flux decline for M0 (Figure 5) when compared to using water at the feed side. Interestingly, the reduction of the water flux on the modified membranes were notably less with approximately 12% (zM-10, 8.8 ± 1.5 LMH), 6% (zM-50, 10.5 ± 1.6 LMH), and 7% (zM-100, 8.7 ± 1.3 LMH). The best water recovery was obtained when using the intermediate molecular weight of PCBMA applied to zM-50. Certainly, the addition of PCBMA molecules inhibits a prominent reduction of the water flux in the presence of BSA foulant molecules. However, the results do not suggest a direct correlation between increasing the PCBMA molecular weight and the reduction of J_w (Figure 5a). Surface roughness plays a significant role when foulant molecules such as BSA are present. Moreover, a surface with higher roughness accelerates the tendency of foulants to adhere. From our AFM characterization (Figure 4), zM-50 resulted with the least average surface roughness of all prepared membranes, hence contributing to the lower flux decline of J_w.

Likewise, J_s decreased for all modified membranes (Figure 5b) when using the BSA foulant solution. Contrary to the control M0 (0.40 ± 0.07 mMH), which J_s augmented nearly 35%, the modified membranes lowered their values (Figure 5b) achieving about 4% reduction for zM-10 (0.26 ± 0.01 mMH), 16% for zM-50 (0.23 ± 0.01 mMH), and 7% for zM-100 (0.27 ± 0.05 mMH). Despite the slight reduction of J_s after the incorporation of PCBMA in the selective layer, there is still no identifiable direct correlation between increasing the PCBMA molecular weight versus a

reduction on the reverse salt flux. Literature shows that zwitterionic polymers have been identified as highly salt sensitive molecules.[3] Henceforth, the electrostatic interactions mechanism between the salt ions and charged groups of PCBMA still play a significant role on the reverse salt flux performance as mentioned earlier in this section.

Thereafter, the fouling behavior was quantified using the flux decline rate (R_t) equation as described in the methodology section. The obtained R_t values revealed outstanding performances for the modified membranes (Figure 5c). This R_t value serves as an indicator to evaluate the resistance of the membrane against fouling.[61] The mid-size molecular weight zM-50 membrane obtained the lowest average R_t resulting in 0.01 ± 0.001, followed by zM-100 (0.05 ± 0.008), and zM-10 (0.13 ± 0.019). The unmodified membrane M0 obtained the highest average decline rate of 0.56 ± 0.071. In a related analysis, the flux recovery ratio (FRR) was calculated for each membrane to assess the capacity of water flux recovery after exposure to BSA foulant solution. Similarly to the R_t trend, the intermediate molecular weight zM-50 resulted with the best performance with FRR values of 96.8 ± 10.4 %, followed by zM-100 (96.5 ± 7.1%), and zM-10 (88.0 ± 0.7%). The unmodified M0 membrane resulted in 50.4 ± 0.5%.

Bacteria and Protein Resistance Results. Different studies have reported that zwitterionic polymers significantly increase the resistance to the attachment of bacteria cells.[62, 63] Living bacteria have the ability to attach on the surface of polymeric material before initiating the biofouling process. In order to mitigate this bacterium-induced biofouling effect, the polymeric coating should provide the conditions to prevent the initial attachment on the surface. Pseudomonas aeruginosa PA01 is an opportunistic human pathogen that can withstand various environmental stresses including conditions of elevated salt.[64] Therefore, this bacterium strain serves as a suitable model for our membrane application intended to desalinate brackish water. To

evaluate the zwitterion coating resistance to bacteria adsorption, we conducted an experiment in which membrane coupons of different molecular weights were incubated for 3 hours with *P. aeruginosa* PA01 expressing a green fluorescent protein to evaluate the effect of using a living organism in a dynamic fouling experiment (Figure 6a). Thereafter, the effect of bacteria adsorption of the different membranes were inspected by measuring the fluorescence intensity (Figure 6b) using a confocal microscope. The acquired images were analyzed using the NIS Elements AR Analysis software Version 5.2.

The results shown in Figure 6a, includes the images of the worst-case scenario in which the most intense fluorescence was observed. The detailed values are summarized in the supporting information Table S3. Interestingly, when normalized against the control M0 PAN membrane, the coating with molecular weight that resulted in the least bacteria adsorption percentage was zM-50 (37.6% ± 10.4). Both PAN surfaces used as the control M0 and zM-10 membranes showed appreciable cell attachment on the surface (M0 = 100% and zM-10 = 32.8 % ±6.2). Moreover, the coating comprising the highest molecular weight, namely zM-100, revealed a relatively higher percentage of bacteria adsorption (61.2 % ± 11.1) when compared to the other two membranes. It is interesting to observe how the molecular weight plays a significant role in preventing the attachment of bacterial cells to the surface. Our results show that using a denser coating of the zwitterionic polymer (zM-100) does not provide adequate bacteria resistance to the membrane.

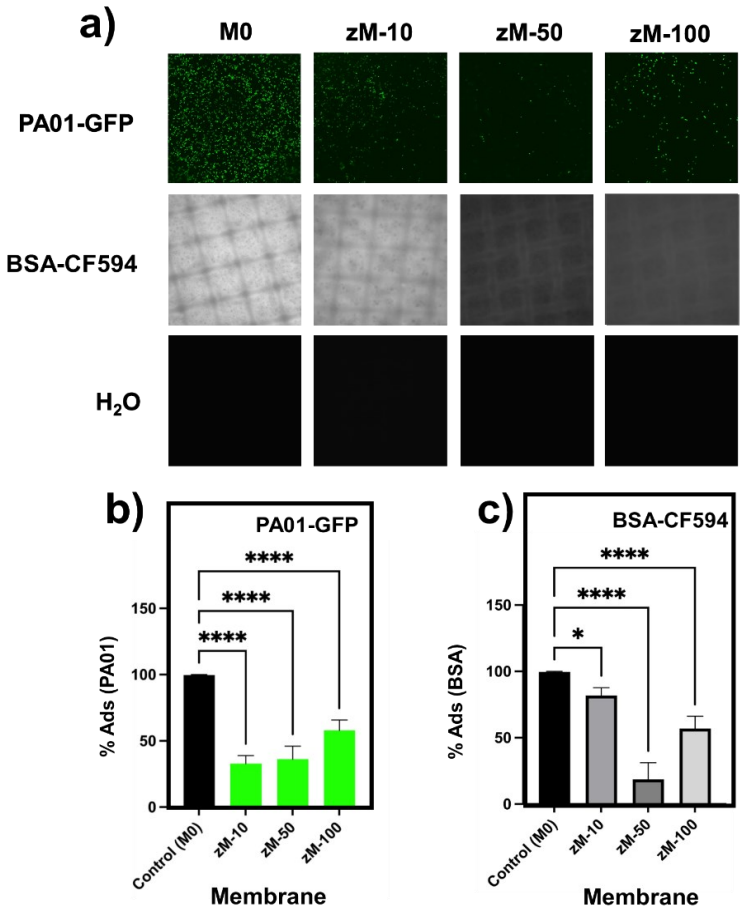

Figure 6. Bacteria and Protein Adsorption Results. a) Fluorescence images of the zwitterion coated TFC membranes after 3h incubation using PA01-GFP and BSA-CF594 solutions. The results are shown in b) the fluorescent intensity graph for the bacteria adsorption experiment and c) the fluorescent intensity graph for the protein adsorption test.

In this case, using a dense or to sparse coating increases the surface roughness that can lead to bacteria adsorption. As discussed earlier, our AFM results (Figure 4) showed that zM-50 obtained the lowest R_a value (4.0 nm) when compared to zM-10 (6.0 nm), zM-100 (5.3 nm), and M0 (7.2 nm). Previous works have recognized how surface roughness also has a negative role on the protein interaction at the surface.[65, 66]Another important aspect is that these experiments were performed at pH 7, where the zM-50 membrane showed the best neutrality of all three.

Continuing with further experiments, the zwitterion coating on the membranes was also tested to measure its resistance to protein adsorption under fixed conditions (Figure 6a, BSA-CF594 and Figure 6c). We conducted this fouling experiment with a BSA bulk solution concentration of 50 ppm and 3 hours of contact time in which the predominant mechanism was protein diffusion. Figure 6a illustrates the images of the fluorescence confocal microscopy with the results for M0, zM-10, zM-50, and zM-100 membranes. In this technique a brighter color in the image indicates a strong fluorescence intensity as a result of the attachment of BSA containing a fluorescent probe (CF594). The resistance of the adsorption onto the polymer's surface was compared against the control membrane (M0) after measuring the fluorescence intensity of adsorbed BSA (Figure 6c). It is important to highlight that the isoelectric point (IEP) of BSA ranges from pH 5.1 to 5.5[67]

Despite of the material hydrophilic nature, the membranes' surfaces revealed different IEP in which the surface charge at neutral pH was positive for zM-10, neutral for zM-50, and negative for zM-100. The surface charge for the M0 control membrane remained neutral along the tested pH range. Contrary to the bacterial experiments, the lowest applied molecular weight zM-10 revealed the highest protein adsorption (zM-10 = 81.8% ± 5.8). This high BSA adsorption in the low molecular weight presumably occurs because of the intrinsic polymer hydrophilicity along with the positive charge which easily attracts the negative surface charge of the protein in aqueous media. Our results suggest that using an intermediate size molecular weight of PCBMA leads to a neutral overall charge at pH 7 which enhances the resistance of protein adhesion on the material's surface with significant difference (zM-50 = 24.4% ± 2.3) against the control membrane. A larger molecular weight also displayed a significant reduction of BSA attachment (zM-100 = 56.9% ± 9.4) against M0 despite the membrane's negative surface charge. Here it is observed that a larger

molecular weight of the polymer promotes material adhesion presumably because the surface roughness of the interface increases thus providing attaching zones for BSA-like proteins.

To further explain it is understood that interfacial thermodynamic[21] governs the molecular interactions at the initial step of the biofouling process that result in the adsorption of organic molecules. Above the interface of a solid/liquid system the molecules will tend to minimize its free energy. Because of being in a condensed state of matter, liquids and solids will have the property of cohesive energy between their molecules.[68] For example when in liquid bulk, water molecules itself will tend to make hydrogen bonds and van der Waals interactions with the nearest neighbor-atoms. However, when there is an interface such as liquid/solid, such molecules are unable to fully form the same bonding dynamics and interactions as when in pure liquid. Non-polar (hydrophobic) molecules that are suspended in water will be repelled because it is difficult to develop polar and hydrogen bonds. In this competition between non-polar and water molecules, the resulting interaction is related to the free energy (ΔG) of the system.[21] Gibbs free energy is a measurement of the system stability and equilibria with respect to a process undertaken at a constant pressure and temperature.[68] Gibbs free energy function is given by the following equation[69]: $\Delta G_{sfe} = \Delta H_{sfe} + T\Delta S_{sfe}$, where the terms ΔG_{sfe} corresponds to the free energy, ΔH_{sfe} to the enthalpy, T to the absolute system temperature, and ΔS_{sfe} the free entropy of adsorption at the interface surface (sfe) of the system. Upon adsorption of non-polar molecules to the water/solid interface, structured water is released within the same aquatic medium which causes also a large increase in entropy (ΔS_{sfe}). The free energy of adsorption would become large and negative ($\Delta G<0$), favoring the process, because of the large entropic term that is associated with the system re-structuring. By employing zwitterions such as PCBMA, it is possible to provide a solvated layer with water molecules that helps in keeping the interfacial energy minimal. Our data in Table 3 for

the interfacial energy validate the fouling resistance behavior of zM-50 by reflecting the lowest IFE value among the modified membranes.

From our results, we are confident to confirm that a higher deposition of living organisms or protein adsorption on the surface will occur in the absence of the zwitterion coating. Indeed, the brush density of the zwitterion coating has a significant role in the cell resistance capacity of the material.

Additional considerations. In order to create a selective thin layer of the thin-film composite (TFC) membranes, it was necessary to prepare a dilute solution of the PEI-PCBMA conjugate. The thermal properties of the conjugated polymers were examined by means of differential scanning calorimetry (DSC) and thermogravimetric analysis (TGA) to confirm no thermal degradation occurred during the heating step of the conjugation synthesis. The resulting curves with increasing temperature of the freeze-dried polymers using the different molecular weights correspond to the second thermal cycle.

The changes in the weight of PCBMA were inspected by thermogravimetric analysis (TGA). The samples were heated from ambient temperature to 550°C at a scan rate of 10 °C/min under argon purging. The TGA thermograms in Figure 7a show the results for the PCBMA modified by PEI grafting to the zwitterion polymer. The modified PCBMA showed two steps of weight loss change before complete decomposition. After an initial weight loss before 100 °C attributable to moisture loss, there is additional weight loss (~32 wt% total) between 100 °C to 300 °C, attributed to an initial partial degradation of the material. Then, an abrupt decay of the curves above 300°C corresponds to severe material decomposition with a weight reduction of ~85.3 wt%. A complete decomposition of the material was observed above 450°C. Our results indicate that major degradation starts to occur at a temperature over 100°C for the different molecular weights of the

conjugated polymers. Moreover, we observed a temperature shift for the thermal degradation above 100°C. This suggests that the final zwitterion coating to be further applied to the membrane surface will be temperature sensitive and may undergo thermal degradation above 100°C.

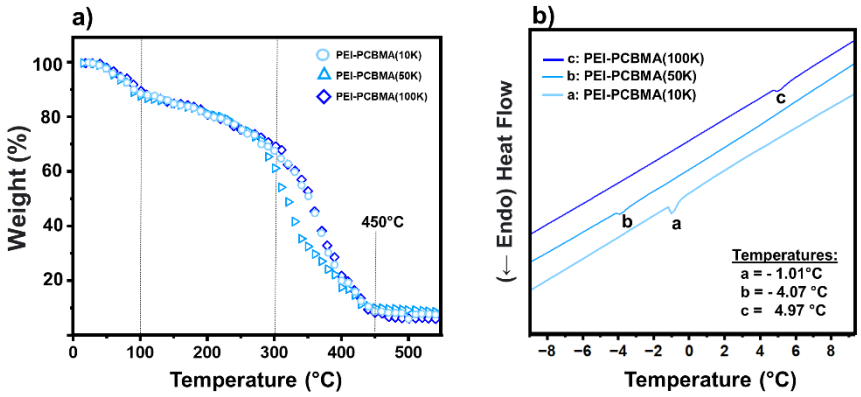

Figure 7. Effect of temperature on the different molecular weights of lyophilized PEI-PCBMA. The results are shown in a) TGA and b) DSC.

DSC experiments were conducted to gain quantitative insight into the thermophysical behavior of the polymers as a function of the molecular weight after the macromolecular modification. The effect of heating the different molecular weight of PEI-PCBMA conjugates resulted in a slight endothermic peak of the DSC signal at temperatures in the vicinity of 0 °C (Figure 7b). The peaks while heating the PEI-PCBMA samples occurred at dissimilar temperatures for the different molecular weights. The observed peak shifts presumably are associated to the loss of non-freezing water molecules that are known to bind strongly with zwitterionic molecules like PCBMA via electrostatic interactions.[20] Results from the obtained thermograms indicate that the conjugated polymers were amorphous, since no melting transitions were observed within the studied range in all cases (Supporting information, Figure S4). Nonetheless, the observed endothermic shifts in the

DSC curves confirm the retained properties of the zwitterion polymer after the conjugation synthesis and are in agreement with previous studies.[70] The polymer was unaffected by the conjugation step and the material is suitable to be further used to construct the zwitterion coated membranes. The application of this technique helps to elucidate the thermal behavior and stability of the conjugated polymers.

Conclusion

In this work, we studied the effect on the forward osmosis performance after applying different molecular weights of PCBMA to coat the surface of various TFC membranes. We aimed to understand the biofouling resistance of the material which will ultimately improve the operational water flux against biofoulants during FO desalination process. Indeed, adding PCBMA to the construction of TFC membranes notably improves the water flux and biofouling resistance properties of the material. In the context of our research quest to probe which molecular weight of the polymer offers the best properties, we concluded that the intermediate size zM-50 of PCBMA has an overall remarkable performance. When using zM-50, higher water permeation was observed. Moreover, the water flux notably improved resulting in an R_t value of 0.01 ± 0.001 (zM-50) upon using a model BSA foulant solution. In contrast, the unmodified control membrane (M0) showed an R_t value of 0.56 ± 0.071 (M0). The data collected for the protein and bacteria experiments revealed that using larger molecular weight does not linearly correlate to higher filtration performance. In terms of resistance to bacteria adhesion, the molecular weight that resulted in the least bacteria adsorption percentage was zM-50 (37.6% ± 10.4). Our results also suggest that using an intermediate size molecular weight of PCBMA leads to a neutral overall charge at pH 7 which enhances the resistance to protein adhesion on the material's surface. Furthermore, this study also revealed that using a denser coating of the zwitterionic polymer (zM-

100) does not provide an adequate bacteria resistance to the membrane, but instead increases the surface roughness that can lead to docking of bacteria into the surface. The improved water flux performance as well as the surface's biofouling resistance feature is attributed to the increased surface hydrophilicity as confirmed by contact angle experiments. Moreover, the specific reverse salt flux J_s/J_w behaves similarly as found to previous works in the literature for zwitterionic membranes. Therefore, it is recommended to conduct further assessment of draw agents that can mitigate the effect of relatively high reverse salt flux (J_s) observed during the FO filtration process. There are still additional physical and chemical properties to continue learning about zwitterionic materials as well as many new membrane-based applications that may benefit from their use. The success of future novel zwitterionic TFC membrane designs stems from its basis on learning and understanding more of these outstanding properties at the molecular level conducted via fundamental research.

4. Acknowledgments

This work was possible thanks to the support from the National Science Foundation Postdoctoral Research Program (NSF-PRP #2112502). Also, thanks to the support of the University of Puerto Rico Rio Piedras campus NSF-CREST Center for Innovation, Research and Education in Environmental Nanotechnology (CIRE2N) Grant Number HRD-1736093 and to NASA MIRO-Puerto Rico Space Partnership for Research, Education and Training (PR-SPRInT) under grant # 80NSSC19M0236. Our sincere appreciation to all personnel in the Molecular Science Research Center (MSRC) for their support and access to the analytical instrumentation, equipment, and research facilities. This research used resources from the Center for Functional Nanomaterials (CFN), which is a U.S. Department of Energy Office of Science User Facility, at Brookhaven National Laboratory under Contract No. DE-SC0012704.

AUTHORS INFORMATION

Corresponding Author, * Prof. Eduardo Nicolau, eduardo.nicolau@upr.edu

Present Addresses

(E.N.) Department of Chemistry, University of Puerto Rico, Rio Piedras Campus, 17 Ave. Universidad Ste. 1701, San Juan, Puerto Rico USA 00925-2537// Molecular Science Research Center, University of Puerto Rico, 1390 Ponce De Leon Ave, Suite 2, San Juan Puerto Rico USA 00931-3346

Author Contributions

The manuscript was written through contributions of all authors. All authors have given approval to the final version of the manuscript.

Notes

The authors declare no competing financial interest.

Supporting Information Available: Additional XPS results, estimated thickness summary, FO membrane stability performance, DSC, and TGA are available.

5. References:

(1) Qin, J.; Ziemann, E.; Bar-Zeev, E.; Bone, S. E.; Liang, Y.; Mauter, M. S.; Herzberg, M.; Bernstein, R. Microporous polyethersulfone membranes grafted with zwitterionic polymer brushes showing microfiltration permeance and ultrafiltration bacteriophage removal. *ACS applied materials & interfaces* **2023**, *15* (14), 18343-18353.

(2) Betancourt-Ponce, M.; Morales-Guzman, C.; Cruz-Tato, P.; Nicolau, E. Probing the Effect of Amine N-Oxide Zwitterionic Polymer Additives in Polysulfone Forward Osmosis Membranes. *ACS Applied Polymer Materials* **2022**, *4* (11), 7966-7975.

(3) Blackman, L. D.; Gunatillake, P. A.; Cass, P.; Locock, K. E. An introduction to zwitterionic polymer behavior and applications in solution and at surfaces. *Chemical Society Reviews* **2019**, *48* (3), 757-770.

(4) Maddah, H.; Chogle, A. Biofouling in reverse osmosis: phenomena, monitoring, controlling and remediation. *Applied Water Science* **2017**, *7*, 2637-2651.

(5) Verma, C.; Dubey, S.; Bose, R.; Alfantazi, A.; Ebenso, E. E.; Rhee, K. Y. Zwitterions and betaines as highly soluble materials for sustainable corrosion protection: Interfacial chemistry and bonding with metal surfaces. *Advances in Colloid and Interface Science* **2024**, 103091.

(6) Yu, W.; Xiong, L.; Teng, J.; Chen, C.; Li, B.; Zhao, L.; Lin, H.; Shen, L. Advances in synthesis and application of amphoteric polymer-based water treatment agents. *Desalination* **2024**, 117280.

(7) Marzullo, P.; Gruttadauria, M.; D'Anna, F. Quaternary Ammonium Salts-Based Materials: A Review on Environmental Toxicity, Anti-Fouling Mechanisms and Applications in Marine and Water Treatment Industries. *Biomolecules* **2024**, *14* (8), 957.

(8) Pintossi, D.; Saakes, M.; Borneman, Z.; Nijmeijer, K. Tailoring the surface chemistry of anion exchange membranes with zwitterions: toward antifouling RED membranes. *ACS Applied Materials & Interfaces* **2021**, *13* (15), 18348-18357.

(9) Zhang, B.; Wang, D.; Wu, Y.; Wang, Z.; Wang, T.; Qiu, J. Modification of the desalination property of PAN-based nanofiltration membranes by a preoxidation method. *Desalination* **2015**, *357*, 208-214.

(10) Li, Q.; Wen, C.; Yang, J.; Zhou, X.; Zhu, Y.; Zheng, J.; Cheng, G.; Bai, J.; Xu, T.; Ji, J. Zwitterionic biomaterials. *Chemical Reviews* **2022**, *122* (23), 17073-17154.

(11) Lodge, T. P.; Hiemenz, P. C. *Polymer Chemistry*; CRC Press, 2020.

(12) Ma, W.; Chen, T.; Nanni, S.; Yang, L.; Ye, Z.; Rahaman, M. S. Zwitterion-functionalized graphene oxide incorporated polyamide membranes with improved antifouling properties. *Langmuir* **2018**, *35* (5), 1513-1525.

(13) Bengani-Lutz, P.; Converse, E.; Cebe, P.; Asatekin, A. Self-assembling zwitterionic copolymers as membrane selective layers with excellent fouling resistance: effect of zwitterion chemistry. *ACS Applied Materials & Interfaces* **2017**, *9* (24), 20859-20872.

(14) Matyjaszewski, K.; Tsarevsky, N. V. Macromolecular engineering by atom transfer radical polymerization. *Journal of the American Chemical Society* **2014**, *136* (18), 6513-6533.

(15) Zhou, L.; Yang, Z.; Pagaduan, J. N.; Emrick, T. Fluorinated zwitterionic polymers as dynamic surface coatings. *Polymer Chemistry* **2023**, *14* (1), 32-36.

(16) Feng, X.; Li, J.; Peng, Y.; Guo, W.; Liang, L.; Zhu, L.; Liu, S.; Ren, L. Zwitterionic polymers as high-performance coatings for hemoperfusion adsorbents and their chemisorption of protein-bound toxins through computational simulations. *Colloids and Surfaces A: Physicochemical and Engineering Aspects* **2024**, *680*, 132710.

(17) Yang, W.; Xue, H.; Li, W.; Zhang, J.; Jiang, S. Pursuing “zero” protein adsorption of poly (carboxybetaine) from undiluted blood serum and plasma. *Langmuir* **2009**, *25* (19), 11911-11916.

(18) Murase, N.; Kurioka, H.; Komura, C.; Ajiro, H.; Ando, T. Synthesis of a novel carboxybetaine copolymer with different spacer lengths and inhibition of nonspecific protein adsorption on its polymer film. *Soft Matter* **2023**, *19* (13), 2330-2338.

(19) Chiao, Y.-H.; Sengupta, A.; Chen, S.-T.; Huang, S.-H.; Hu, C.-C.; Hung, W.-S.; Chang, Y.; Qian, X.; Wickramasinghe, S. R.; Lee, K.-R. Zwitterion augmented polyamide membrane for improved forward osmosis performance with significant antifouling characteristics. *Separation and Purification Technology* **2019**, *212*, 316-325.

(20) Chiao, Y.-H.; Sengupta, A.; Ang, M. B. M. Y.; Chen, S.-T.; Haan, T. Y.; Almodovar, J.; Hung, W.-S.; Wickramasinghe, S. R. Application of zwitterions in forward osmosis: A short review. *Polymers* **2021**, *13* (4), 583.

(21) Kardela, J. H.; Millichamp, I. S.; Ferguson, J.; Parry, A. L.; Reynolds, K. J.; Aldred, N.; Clare, A. S. Nonfreezable water and polymer swelling control the marine antifouling performance of polymers with limited hydrophilic content. *ACS applied materials & interfaces* **2019**, *11* (33), 29477-29489.

(22) Liu, Y.; Zhang, D.; Ren, B.; Gong, X.; Xu, L.; Feng, Z.-Q.; Chang, Y.; He, Y.; Zheng, J. Molecular simulations and understanding of antifouling zwitterionic polymer brushes. *Journal of materials chemistry B* **2020**, *8* (17), 3814-3828.

(23) Wu, J.; He, C.; He, H.; Cheng, C.; Zhu, J.; Xiao, Z.; Zhang, H.; Li, X.; Zheng, J.; Xiao, J. Importance of zwitterionic incorporation into polymethacrylate-based hydrogels for simultaneously improving optical transparency, oxygen permeability, and antifouling properties. *Journal of Materials Chemistry B* **2017**, *5* (24), 4595-4606.

(24) Li, B.; Yuan, Z.; Zhang, P.; Sinclair, A.; Jain, P.; Wu, K.; Tsao, C.; Xie, J.; Hung, H. C.; Lin, X. Zwitterionic nanocages overcome the efficacy loss of biologic drugs. *Advanced Materials* **2018**, *30* (14), 1705728.

(25) Chou, Y.-N.; Sun, F.; Hung, H.-C.; Jain, P.; Sinclair, A.; Zhang, P.; Bai, T.; Chang, Y.; Wen, T.-C.; Yu, Q. Ultra-low fouling and high antibody loading zwitterionic hydrogel coatings for sensing and detection in complex media. *Acta biomaterialia* **2016**, *40*, 31-37.

(26) Cai, T.; Yang, W. J.; Neoh, K.-G.; Kang, E.-T. Poly (vinylidene fluoride) membranes with hyperbranched antifouling and antibacterial polymer brushes. *Industrial & engineering chemistry research* **2012**, *51* (49), 15962-15973.

(27) Craig, R. A.; McCoy, C. P. Light-triggered anti-infective surfaces. *Antimicrobial Coatings and Modifications on Medical Devices* **2017**, 241-266.

(28) Anbarasan, R.; Ranchani, A. A. J.; Liu, Y. C.; Tung, K. L. Synthesis and Characterization of Zwitter ion Functionalized Polysulfone Membrane. *ChemistrySelect* **2022**, *7* (33), e202200406.

(29) Wang, M.; Huang, T.; Shan, M.; Sun, M.; Liu, S.; Tang, H. Zwitterionic Tröger's Base Microfiltration Membrane Prepared via Vapor-Induced Phase Separation with Improved Demulsification and Antifouling Performance. *Molecules* **2024**, *29* (5), 1001.

(30) Fu, Y.; Wang, Y.; Huang, L.; Xiao, S.; Chen, F.; Fan, P.; Zhong, M.; Tan, J.; Yang, J. Salt-responsive "killing and release" antibacterial surfaces of mixed polymer brushes. *Industrial & Engineering Chemistry Research* **2018**, *57* (27), 8938-8945.

(31) Niu, J.; Wang, H.; Chen, J.; Chen, X.; Han, X.; Liu, H. Bio-inspired zwitterionic copolymers for antifouling surface and oil-water separation. *Colloids and Surfaces A: Physicochemical and Engineering Aspects* **2021**, *626*, 127016.

(32) Zhang, Y.; Liu, Y.; Ren, B.; Zhang, D.; Xie, S.; Chang, Y.; Yang, J.; Wu, J.; Xu, L.; Zheng, J. Fundamentals and applications of zwitterionic antifouling polymers. *Journal of Physics D: Applied Physics* **2019**, *52* (40), 403001.

(33) Pazol, J.; Cruz-Tato, P.; Nicolau, E. Characterization of a Model Bioreactive Membrane for the Simultaneous Separation and Hydrolysis of Lipopolysaccharides. *ACS Applied Engineering Materials* **2023**, *1* (6), 1684-1697.

(34) Sun, J.; Zeng, F.; Jian, H.; Wu, S. Grafting zwitterionic polymer chains onto PEI as a convenient strategy to enhance gene delivery performance. *Polymer Chemistry* **2013**, *4* (24), 5810-5818.

(35) Chiao, Y.-H.; Chen, S.-T.; Patra, T.; Hsu, C.-H.; Sengupta, A.; Hung, W.-S.; Huang, S.-H.; Qian, X.; Wickramasinghe, R.; Chang, Y. Zwitterionic forward osmosis membrane modified by fast second interfacial polymerization with enhanced antifouling and antimicrobial properties for produced water pretreatment. *Desalination* **2019**, *469*, 114090.

(36) Ang, M. B. M. Y.; Ji, Y.-L.; Huang, S.-H.; Tsai, H.-A.; Hung, W.-S.; Hu, C.-C.; Lee, K.-R.; Lai, J.-Y. Incorporation of carboxylic monoamines into thin-film composite polyamide membranes to enhance nanofiltration performance. *Journal of Membrane Science* **2017**, *539*, 52-64.

(37) Idrees, M. F.; Tariq, U. Enhancing chlorine resistance in polyamide membranes with surface & structure modification strategies. *Water Supply* **2022**, *22* (2), 1199-1215.

(38) Wang, K.; Wang, X.; Januszewski, B.; Liu, Y.; Li, D.; Fu, R.; Elimelech, M.; Huang, X. Tailored design of nanofiltration membranes for water treatment based on synthesis–property–performance relationships. *Chemical Society Reviews* **2022**, *51* (2), 672-719.

(39) Maruf, S. H.; Greenberg, A. R.; Ding, Y. Influence of substrate processing and interfacial polymerization conditions on the surface topography and permselective properties of surface-patterned thin-film composite membranes. *Journal of membrane science* **2016**, *512*, 50-60.

(40) Hanif, M. A.; Ibrahim, N.; Dahalan, F. A.; Md. Ali, U. F.; Hasan, M.; Azhari, A. W.; Jalil, A. A. Microplastics in facial cleanser: extraction, identification, potential toxicity, and continuous-flow removal using agricultural waste–based biochar. *Environmental Science and Pollution Research* **2023**, *30* (21), 60106-60120.

(41) Jafari, M.; Jung, J. The change in contact angle at unsaturated CO2-water conditions: Implication on geological carbon dioxide sequestration. *Geochemistry, Geophysics, Geosystems* **2016**, *17* (10), 3969-3982.

(42) Xiao, M.; Yang, F.; Im, S.; Dlamini, D. S.; Jassby, D.; Mahendra, S.; Honda, R.; Hoek, E. M. Characterizing surface porosity of porous membranes via contact angle measurements. *Journal of Membrane Science Letters* **2022**, *2* (1), 100022.

(43) Lamour, G.; Hamraoui, A.; Buvailo, A.; Xing, Y.; Keuleyan, S.; Prakash, V.; Eftekhari-Bafrooei, A.; Borguet, E. Contact angle measurements using a simplified experimental setup. *Journal of chemical education* **2010**, *87* (12), 1403-1407.

(44) Williams, D. L.; Kuhn, A. T.; Amann, M. A.; Hausinger, M. B.; Konarik, M. M.; Nesselrode, E. I. Computerised measurement of contact angles. *Galvanotechnik* **2010**, *101* (11), 2502.

(45) Wu, S. Calculation of interfacial tension in polymer systems. In *Journal of Polymer Science Part C: Polymer Symposia*, 1971; Wiley Online Library: Vol. 34, pp 19-30.

(46) Castrillón, S. R.-V.; Lu, X.; Shaffer, D. L.; Elimelech, M. Amine enrichment and poly (ethylene glycol)(PEG) surface modification of thin-film composite forward osmosis membranes for organic fouling control. *Journal of Membrane Science* **2014**, *450*, 331-339.

(47) Guillen, G. R.; Pan, Y.; Li, M.; Hoek, E. M. Preparation and characterization of membranes formed by nonsolvent induced phase separation: a review. *Industrial & Engineering Chemistry Research* **2011**, *50* (7), 3798-3817.

(48) Zhao, W.; Ye, Q.; Hu, H.; Wang, X.; Zhou, F. Grafting zwitterionic polymer brushes via electrochemical surface-initiated atomic-transfer radical polymerization for anti-fouling applications. *Journal of Materials Chemistry B* **2014**, *2* (33), 5352-5357.

(49) Koushkbaghi, S.; Jafari, P.; Rabiei, J.; Irani, M.; Aliabadi, M. Fabrication of PET/PAN/GO/Fe3O4 nanofibrous membrane for the removal of Pb (II) and Cr (VI) ions. *Chemical Engineering Journal* **2016**, *301*, 42-50.

(50) Xiao, S.; Zhang, Y.; Shen, M.; Chen, F.; Fan, P.; Zhong, M.; Ren, B.; Yang, J.; Zheng, J. Structural dependence of salt-responsive polyzwitterionic brushes with an anti-polyelectrolyte effect. *Langmuir* **2018**, *34* (1), 97-105.

(51) Shen, L.; Zhang, X.; Zuo, J.; Wang, Y. Performance enhancement of TFC FO membranes with polyethyleneimine modification and post-treatment. *Journal of Membrane Science* **2017**, *534*, 46-58.

(52) Pavia, D. L.; Lampman, G. M.; Kriz, G. S.; Vyvyan, J. A. *Introduction to spectroscopy*; Cengage learning, 2014.

(53) Kishore Chand, A. A.; Bajer, B.; Schneider, E. S.; Mantel, T.; Ernst, M.; Filiz, V.; Glass, S. Modification of polyacrylonitrile ultrafiltration membranes to enhance the adsorption of cations and anions. *Membranes* **2022**, *12* (6), 580.

(54) Mantel, T.; Glass, S.; Usman, M.; Lyberis, A.; Filiz, V.; Ernst, M. Adsorptive dead-end filtration for removal of Cr (vi) using novel amine modified polyacrylonitrile ultrafiltration membranes. *Environmental Science: Water Research & Technology* **2022**, *8* (12), 2981-2993.

(55) Aktij, S. A.; Firouzjaei, M. D.; Haddadi, S. A.; Karami, P.; Taghipour, A.; Yassari, M.; Asad, A. A.; Pilevar, M.; Jafarian, H.; Arjmand, M. Metal-organic frameworks' latent potential as High-Efficiency osmotic power generators in Thin-Film nanocomposite membranes. *Chemical Engineering Journal* **2024**, *481*, 148384.

(56) Liao, C.; Zhao, J.; Yu, P.; Tong, H.; Luo, Y. Synthesis and characterization of SBA-15/poly (vinylidene fluoride)(PVDF) hybrid membrane. *Desalination* **2010**, *260* (1-3), 147-152.

(57) Murugaboopathy, S.; Matsuoka, H. Salt-dependent surface activity and micellization behaviour of zwitterionic amphiphilic diblock copolymers having carboxybetaine. *Colloid and Polymer Science* **2015**, *293*, 1317-1328.

(58) Ni, L.; Meng, J.; Geise, G. M.; Zhang, Y.; Zhou, J. Water and salt transport properties of zwitterionic polymers film. *Journal of membrane science* **2015**, *491*, 73-81.

(59) Zheng, K.; Zhou, S. Fabrication of a novel cyanoethyl cellulose substrate for thin-film composite forward osmosis membrane. *Blue Green Systems* **2019**, *1* (1), 18-32.

(60) Song, H.; Liu, J.; Wu, D. Performance comparison between TFC-ES membranes and aquaporin membranes for dairy wastewater reclamation. *Desalination and Water Treatment* **2018**, *109*, 28-35.

(61) Zhu, J.; Zhou, S.; Li, M.; Xue, A.; Zhao, Y.; Peng, W.; Xing, W. PVDF mixed matrix ultrafiltration membrane incorporated with deformed rebar-like Fe3O4–palygorskite nanocomposites to enhance strength and antifouling properties. *Journal of Membrane Science* **2020**, *612*, 118467.

(62) Huang, L.; Zhang, L.; Xiao, S.; Yang, Y.; Chen, F.; Fan, P.; Zhao, Z.; Zhong, M.; Yang, J. Bacteria killing and release of salt-responsive, regenerative, double-layered polyzwitterionic brushes. *Chemical Engineering Journal* **2018**, *333*, 1-10.

(63) Cheng, G.; Zhang, Z.; Chen, S.; Bryers, J. D.; Jiang, S. Inhibition of bacterial adhesion and biofilm formation on zwitterionic surfaces. *Biomaterials* **2007**, *28* (29), 4192-4199.

(64) Woodcock, S. D.; Syson, K.; Little, R. H.; Ward, D.; Sifouna, D.; Brown, J. K.; Bornemann, S.; Malone, J. G. Trehalose and α-glucan mediate distinct abiotic stress responses in Pseudomonas aeruginosa. *PLoS Genetics* **2021**, *17* (4), e1009524.

(65) Werber, J. R.; Osuji, C. O.; Elimelech, M. Materials for next-generation desalination and water purification membranes. *Nature Reviews Materials* **2016**, *1* (5), 1-15.

(66) Liu, C.; Lee, J.; Small, C.; Ma, J.; Elimelech, M. Comparison of organic fouling resistance of thin-film composite membranes modified by hydrophilic silica nanoparticles and zwitterionic polymer brushes. *Journal of Membrane Science* **2017**, *544*, 135-142.

(67) TJ, P. Serum albumin. *Adv Protein Chem* **1985**, *37*, 161-245.

(68) Tsujii, K. *Surface Activity: Principles, Phenomena, and Applications*; Academic Press, 1998.

(69) Smith, J. M.; Van Ness, H. C.; Abbott, M. *Introduction to Chemical Engineering Thermodynamics*; McGraw-Hill Education, 2005.

(70) Wang, Z.; Yuan, L.; Trenor, N. M.; Vlaminck, L.; Billiet, S.; Sarkar, A.; Du Prez, F. E.; Stefik, M.; Tang, C. Sustainable thermoplastic elastomers derived from plant oil and their "click-coupling" via TAD chemistry. *Green chemistry* **2015**, *17* (7), 3806-3818.